

Article

CO₂ Compression and Liquefaction Processes Using a Distillation Column for the Flexible Operation of Transportation

Semie Kim ¹, Pyeong-Gon Jung ¹, Young-II Lim ^{1,*}, Hyojoon Kim ² and Hung-Man Moon ²

¹ CoSPE, Department of Chemical Engineering, Hankyong National University, Jungang-ro 327, Anseong-si 17579, Gyeonggi-do, Republic of Korea; kimsemie04@hknu.ac.kr (S.K.); zkjxc975@hknu.ac.kr (P.-G.J.)

² A-ONE Co., Ltd., 35, Jeongwangcheondong-ro 94beon-gil, Danwon-gu, Ansan-si 15415, Gyeonggi-do, Republic of Korea; onam117@naver.com (H.K.); moon@dsaone.co.kr (H.-M.M.)

* Correspondence: limyi@hknu.ac.kr

Abstract: Impurities in the CO₂ stream should be removed to prevent eventual phase changes in CO₂ transportation because a two-phase flow caused by the phase change in the pipeline necessitates additional overpressure and can induce equipment damage. In this study, CO₂ compression and liquefaction (CCL) processes with a distillation column were used to remove non-condensable impurities and were compared with those with a flash. Three different feeds with a flow rate of 50.1 t/h (400,500 t/y) were supplied to the CCL processes and compressed to 65 bar to gauge pressure (barg) and 20 °C. Although the CO₂ mixtures obtained through dehydration and flashing met the purity requirements for transportation and storage recommended in literature, the flash-separated CO₂ product at 65 barg demonstrated the coexistence of gas and liquid phases, which restricted the temperature window for liquid CO₂ transportation. When the distillation column was used instead of the flash, the operating temperature window at 65 barg widened by 3–6 °C owing to the high purity of CO₂. However, the levelized cost of CO₂ liquefaction (LCCL) increased by 2–4 \$/t-CO₂ varying with the feed purity because the distillation column consumed more cooling and heating duties than the flash. This study highlighted that a two-phase flow existed under certain operating conditions despite a high purity of CO₂ (over 97 mol%), and the distillation column enhanced the operability of liquid CO₂ transportation.

Keywords: CO₂ compression and liquefaction; CO₂ transportation; two-phase flow; distillation column; phase envelope; techno-economic analysis (TEA)



Citation: Kim, S.; Jung, P.-G.; Lim, Y.-I.; Kim, H.; Moon, H.-M. CO₂ Compression and Liquefaction Processes Using a Distillation Column for the Flexible Operation of Transportation. *Processes* **2024**, *12*, 115. <https://doi.org/10.3390/pr12010115>

Academic Editors: Federica Raganati and Paola Ammendola

Received: 14 December 2023

Revised: 29 December 2023

Accepted: 30 December 2023

Published: 2 January 2024



Copyright: © 2024 by the authors. Licensee MDPI, Basel, Switzerland. This article is an open access article distributed under the terms and conditions of the Creative Commons Attribution (CC BY) license (<https://creativecommons.org/licenses/by/4.0/>).

1. Introduction

To meet the global energy demands, CO₂ emissions from fossil fuels continue to increase [1]. CO₂ capture and storage (CCS) is crucial for mitigating the CO₂ concentration in the atmosphere for sustainable development considering the environment [2,3]. The CCS technology consists of CO₂ capture (using absorption, adsorption, cryogenic purification, and membranes), CO₂ compression and liquefaction (CCL), CO₂ transportation (via trucks, ships, and pipelines), and sequestration in the ground, sea, and depleted reservoirs [4–6]. The composition of a CO₂-rich mixture captured from combustion processes depends on the fuel type (e.g., coal, natural gas, oil, and biomass) and capture technologies, such as pre-, post-, and oxy-combustion [7–9]. The CO₂ mixture contains various impurities such as H₂O, H₂S, CO, SO₂, Ar, H₂, CH₄, O₂, N₂, and NH₃ [10,11]. Water is produced by the combustion of fossil fuels. H₂ and CH₄ are the main impurities in steam methane reforming (SMR) for H₂ production. O₂ remains in the flue gas of oxy-combustion plants [12].

The purity of the CO₂ mixture for pipeline transportation and storage is determined by considering the pipeline corrosion, undesirable side reactions, as well as environmental

and economic factors [7,13,14]. Table 1 lists the recommended CO₂ compositions [7,10]. The European project DYNAMIS (2008) proposed guidelines regarding the quality of CO₂ for pipeline transportation [15], recommending a CO₂ purity of greater than 95.5 vol% and a water content below 500 ppm-volume based (ppm_v) [10]. NETL (2012) recommended purity limits for pipeline transportation and saline reservoir sequestration, indicating that the total amount of non-condensable components (N₂, O₂, Ar, CH₄, CO, and H₂) was less than 4 vol%, and the water content was less than 300 ppm-weight based (ppm_{wt}) [10]. Abbas et al. (2013) reported the purification limits for the geological storage of CO₂, recommending a CO₂ purity of greater than 90 vol% and a water content below 500 ppm_v [7]. The non-condensable gas content was limited to less than 4 vol% to avoid a two-phase flow in the pipeline transportation [7,10], increase the storage capacity, and decrease the compressor duty required for geological storage [11].

Table 1. Recommended purity of CO₂ mixtures for pipeline transportation and geological storage [7,10].

Component	Purity Limits for Pipeline		Purity Limits for Geological Storage
	DYNAMIS	NETL	
CO ₂	>95.5 vol%	95 vol%	>90 vol%
H ₂ O	500 ppm _v	300 ppm _{wt}	<500 ppm _v
H ₂ S	200 ppm _v	0.01 vol%	<1.5%
CO	2000 ppm _v	35 ppm _v	
CH ₄	Aquifer < 4 vol%	4 vol%	
N ₂	<4 vol%	4 vol%	<4 vol% (all non-condensable gasses)
Ar	(all non-condensable gasses)	4 vol%	
H ₂		4 vol%	
O ₂	-	4 vol%	
NO _x	-	100 ppm _v	<200 ppm _v
SO _x	-	100 ppm _v	<200 ppm _v
NH ₃	-	50 ppm _v	

The strength of the pipelines must be increased to minimize the possibility of ductile fracture because N₂, CH₄, and H₂ have low critical temperatures [8]. Toxic components such as CO and H₂S pose safety concerns owing to exposure or leakage from the pipelines and geological sequestration [11,16]. Despite the purity limits of CO₂ being satisfied, small amounts of impurities can affect the phase behavior during transportation, storage, and injection [13,16,17].

Pure CO₂ is liquefied between the triple (5.2 bar, −56.5 °C) and critical points (73.8 bar, 31.1 °C) [18]. A CO₂ stream with impurities has an increased critical pressure (P_c) and is liquefied at a higher pressure than pure CO₂, which results in an increased power consumption [16]. Additionally, the pressure drop of an impure CO₂ stream is higher than that of pure CO₂ during pipeline transportation [19]. For a CO₂ stream containing impurities, the pipeline pressure should be increased to prevent the phase change [16], and the liquefying temperature should be lower than that of pure CO₂ owing to its low critical temperature (T_c).

Brownsort et al. (2019) reported that 99.7 vol% of CO₂ is required to prevent the formation of dry ice during ship transportation [20]. Peletiri et al. (2019) analyzed the effect of impurities on CO₂ fluid behavior, such as the density, viscosity, phase envelope, and critical point [8]. Goos et al. (2011) compared the phase envelopes of CO₂ mixtures containing 5 and 10 mol% N₂ during a CO₂ compression process [21]. To remove volatile gases from an impure CO₂ stream, a distillation column was used instead of a flash for the CO₂ conditioning process for both pipeline and ship transport [13]. Xu et al. (2014) proposed a distillation column to produce high-purity CO₂ from mixtures with CO₂, N₂, O₂, and Ar to satisfy the specifications for CO₂ transportation and storage [22].

Seo et al. (2016) compared the cost of CO₂ liquefaction processes, including a liquefaction unit, storage tanks in the intermediate terminal, a CO₂ carrier, and pumps,

demonstrating an optimal liquefaction pressure of 15 bar ($-27\text{ }^{\circ}\text{C}$) for ship-based CCS chains [23]. Adu et al. (2020) evaluated the CO₂ avoidance cost (\$72–\$94/t-CO₂) in CO₂ capture and compression processes from 550 MW coal and natural gas-fired power plants [24]. The CO₂ liquefaction cost under the purity requirements was assessed for pure and impure CO₂ feeds at different pressures [25]. Gong et al. (2022) compared the total capital investment (TCI) and utility costs for open- and closed-cycle CO₂ liquefaction processes at 7 and 15 bar for transportation [26]. Although these studies demonstrated scientific and technological advances in CCL, they failed to present the extent to which the CCL process with a distillation column removing impurities from the CO₂-rich mixture improved the operability of pipeline and ship transportation. They also overlooked the increase in the CO₂ liquefaction costs for the removal of impurities using distillation columns.

In this study, a process flow diagram (PFD) of CCL processes involving a flash or distillation column is presented, which focuses on the impurity removal from three different CO₂-rich mixtures for stable CO₂ transportation. The operating ranges that prevent the two-phase flow in CO₂ transportation were investigated by analyzing the phase envelopes of liquefied CO₂ produced from the bottom of the flash or distillation column. The leveled cost of CO₂ compression and liquefaction (LCCL) was evaluated to examine the economic impact of the impurity removal from CO₂-rich mixtures. This study demonstrated that a CCL process equipped with a distillation column improves the operability of CO₂ transportation by removing non-condensable gases and preventing two-phase flow.

2. Process Description of CO₂ Compression and Liquefaction

A CO₂-rich mixture (50.068 t/h or 400,544 t/y) was supplied to a CCL process in an intermediate terminal for transportation and sequestration. The supplied CO₂ mixture was assumed to be at 25 °C and 15 bar to gauge pressure (barg). Three CO₂-rich mixtures satisfying the purity limits of DYNAMIS (see Table 1), except H₂O, were considered as the CO₂ feed: (i) CO₂ captured from an SMR plant (Feed 1), (ii) CO₂ captured from post-combustion with a main impurity of N₂ (Feed 2), and (iii) CO₂ containing H₂ as an impurity (Feed 3).

Table 2 lists the temperature (T), pressure (P), mass flow rate (F), and composition (y_i) of the three feeds. Feed 1 contained 99.13 mol% CO₂, 0.7 mol% non-condensable gas (0.61 mol% H₂, 0.09 mol% CH₄), 200 ppm CO, and 1500 ppm H₂O, which was provided by a Korean company. The compositions of Feeds 2 and 3 were 97 mol% CO₂, 1500 ppm H₂O, and 2.85 mol% N₂ or H₂, respectively, which were used to investigate the possibility of the two-phase flow in CO₂ transportation at various operating conditions.

Table 2. Inlet conditions of three CO₂-rich feeds.

	Feed 1	Feed 2	Feed 3
Temperature (T , °C)	25	25	25
Pressure (P , barg)	15	15	15
Mass flow rate (F , kg/hr)	50,068	50,068	50,068
Mole fraction (y_i)			
CO ₂	0.9913	0.9700	0.9700
CO	0.0002	0.0000	0.0000
H ₂	0.0061	0.0000	0.0285
CH ₄	0.0009	0.0000	0.0000
H ₂ O	0.0015	0.0015	0.0015
N ₂	0.0000	0.0285	0.0000
Total	1.0000	1.0000	1.0000

ASPEN Plus V14 (ASPEN Tech., Bedford, MA, USA, 2022) was used to conceptually design the CCL process. The Peng–Robinson (PR) equation of state (EOS), which is a cubic equation of state with binary interaction parameters accounting for the non-ideality of the

fluid mixture, was selected to predict the thermodynamic properties of the fluids [27,28]. The PR EOS is frequently used for the phase equilibria of CO₂ mixtures [29,30].

Figure 1 presents the phase envelopes obtained from the PR EOS, as well as the P_c and T_c values of pure CO₂ [29] and a CO₂ mixture with 14 mol% N₂ [31]. The PR EOS was calculated using the density marching method [32], which is appropriate for calculating the phase envelope around the critical point (T_c, P_c), which was located at the edge of the phase envelope on the P and T plane (PT phase envelope). The left line of the critical point indicates the bubble points and the right line indicates the dew points. Two phases appeared between the bubble and dew points within certain ranges of P and T , as illustrated in Figure 1. The gas and liquid phases did not coexist for pure CO₂ (thick black solid line) below the critical point, whereas the two phases appeared for the CO₂ mixture with 14 mol% N₂ (thin blue solid line).

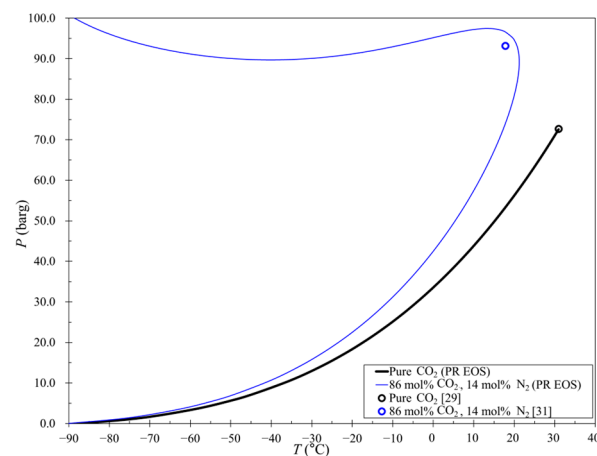


Figure 1. Phase envelopes obtained from the PR EOS. Critical pressure (P_c) and temperature (T_c) of pure CO₂ (thick black solid line), CO₂ mixtures with 14 mol% N₂ (thin blue solid line), and experimental points (circles) are shown.

The experimentally measured critical points are indicated by the circles. The mean error of P_c between the PR EOS and experimental values was 0.55%, whereas that of T_c was 6.40%. The critical points obtained from the PR EOS sufficiently agreed with the experimental data. The T_c value was lower and the P_c value was higher for the CO₂ mixtures containing N₂, when compared to those of pure CO₂. Li et al. (2015) used the PR EOS to explain the effect of the impurities in CO₂ mixtures on the phase change [10]. Babar et al. (2018) reported that the deviation between the PR EOS and experimental data in a CO₂-CH₄ binary system was $\pm 3\%$ for the three-phase locus [33]. Peletiri et al. (2017) selected the PR EOS to identify the pressure drop and phase change in pipeline transportation of CO₂ flows containing impurities [34].

The CCL process includes a temperature swing adsorption (TSA) unit for H₂O removal, a two-stage compressor and cooler, cooling water and chiller systems, an R134a refrigerant cycle system, and a flash or distillation column for non-condensable gas removal, as shown in Figures 2 and 3. The CO₂ feed first entered a TSA unit for dehydration to 49 ppm_v H₂O, which is the recommendation for CO₂ transportation and storage based on the guideline [35]. The pressure drop in the TSA unit was 2 bar and the dewatered CO₂ stream exited at 13 barg and 25 °C. The CO₂ stream was compressed to 25.5 and 66.2 barg using the first and second compressors, respectively. The efficiencies of the compressors were set to 72%. The temperature that was elevated by compression was lowered to 40 °C by using the cooling water system, where the pressure drop in the coolers was 0.5 bar. The cooling tower was operated at 32–37 °C, where the heat loss was 5%.

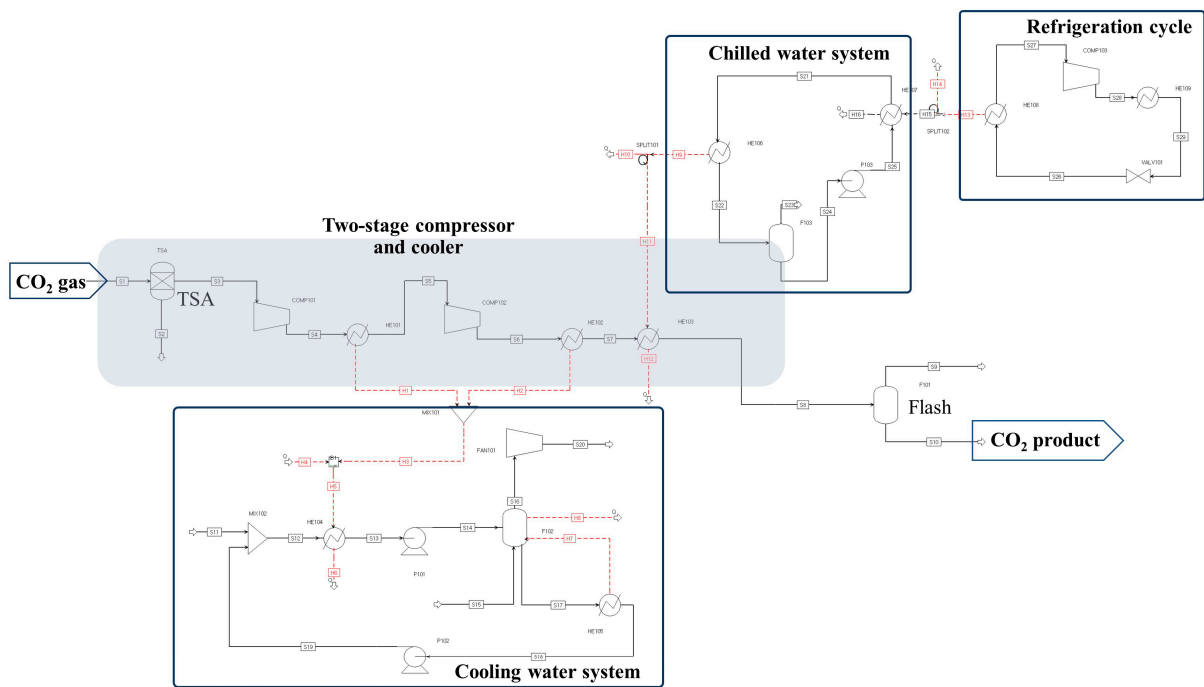


Figure 2. Process flow diagram (PFD) of a CO₂ compression and liquefaction (CCL) process with a flash.

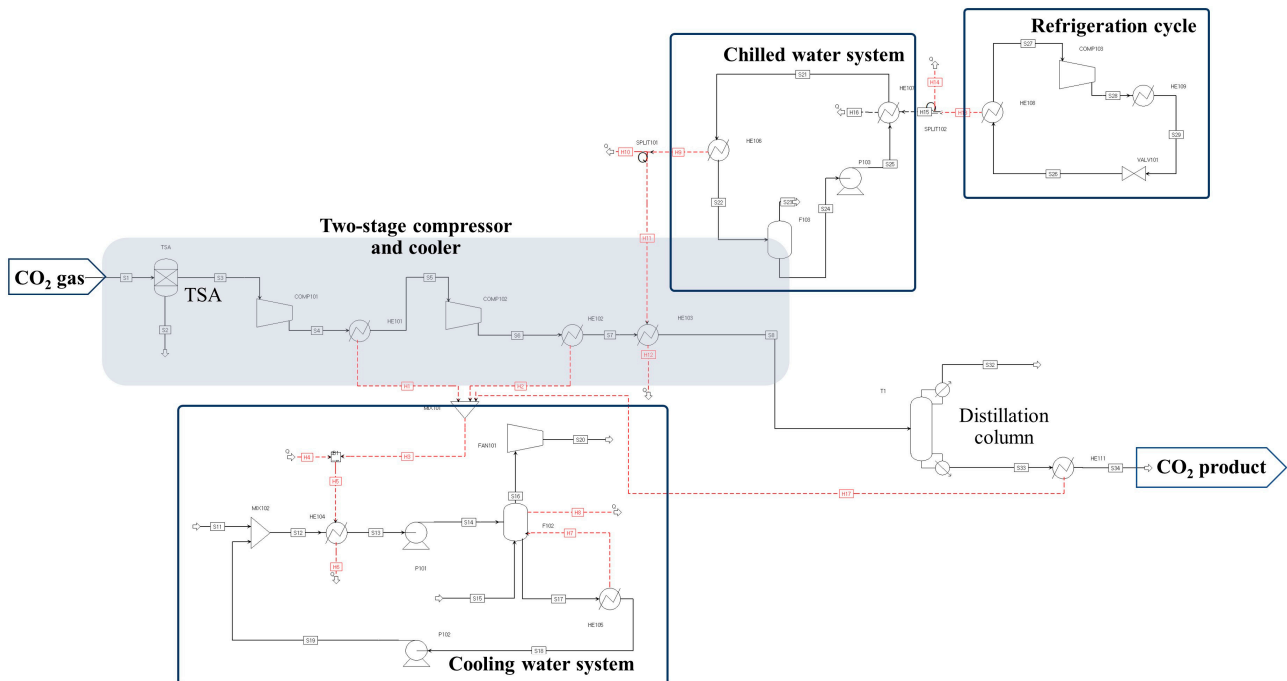


Figure 3. Process flow diagram (PFD) of a CO₂ compression and liquefaction (CCL) process with a distillation column.

The CO₂ stream at 65.7 barg and 40 °C was cooled once again to 20 °C using a chiller. The chilled water system, which was capable in lowering the temperature of a fluid to 20 °C, was operated at 6–12 °C. The pressure drop in the chilled water cooler was 0.7 bar. For the production of chilled water at 6 °C in the chilled water system, a refrigeration cycle with an R134a refrigerant was used, which was operated at −2.9–35 °C and 1.6–7.9 barg [36]. The

leakage fraction of the valves in the refrigeration cycle and chilled water system was set to 0.0001.

Liquefied CO₂ was produced at the bottom of the flash or distillation column. The flash was operated at 65 barg and 20 °C. The eight-stage distillation column was used, where the feed was supplied to the third stage and the reflux ratio was 7.04 for Feeds 1 and 2, and 9.97 for Feed 3. The operating pressure of the distillation column ranged from 65 to 65.1 barg. A chiller was used to lower the condenser temperature of the distillation column; chiller from the chilled water system at 17.9 °C for Feed 1, and chiller from the refrigeration cycle at 2.7 and 3.3 °C for Feeds 2 and 3, respectively. Low-pressure steam was supplied to the reboiler of the distillation column. A chiller was used to adjust the temperature of the liquefied CO₂ product to 20 °C at the bottom of the distillation column. The CO₂ recovery of the distillation column was set to 93%, which was commonly used in other studies [13,22]. The liquefied CO₂ was produced at 65 barg and 20 °C from both the flash and distillation column.

3. Methodology of Techno-Economic Analysis (TEA)

A techno-economic analysis (TEA) method [37,38] was employed to evaluate the economic feasibility of the CCL processes. An Aspen Process Economic Analyzer V14 (ASPEN Tech., Bedford, MA, USA, 2022) was used to calculate the total direct and indirect costs (TDIC) of each equipment, which included 4% for instrumentation and control, 9% for piping, and 4% for electrical systems of the total equipment cost [38]. The fixed capital investment (FCI) was obtained by adding the TDIC and project contingency (PC), which was set to 10% of the TDIC. The working capital (WC) was assumed to be 5% of the FCI, and the total capital investment (TCI) was the sum of the FCI and WC.

The total production cost (TPC) was calculated as the sum of the raw materials, utilities, and fixed costs. The raw material cost of CO₂ was ignored, which was directly supplied by the CO₂ capturing unit. The utility costs included those used for the cooling water, chiller, R134a refrigerant, LNG for steam, and electricity for compressors and pumps. The fixed cost consisted of the operating labor cost, maintenance cost (2% of FCI), operating charges (25% of labor cost), plant overhead (70% of labor cost), and general and administrative costs (8% of labor cost) [38–40].

Several economic assumptions were applied for the calculation of TPC: (i) the plant operates 8000 h per year, (ii) the plant life (L_p) and depreciation period is 30 years [40], (iii) the debt-to-equity ratio is 70% of the TCI [4], (iv) the inflation rate (α), corporation tax rate (β), and interest rate (γ) are 2%/y, 20%, and 6%/y, respectively [38]; (v) the supervisors and workers receive wages of \$400,000 and \$640,000 per year, respectively, (vi) a total of 16 workers and 5 supervisors work with three shifts a day [41], (vii) the operating cost of TSA is \$0.371 per ton of the inlet stream [42], (viii) the electricity and LNG prices are 98 \$/MWh_e and 26.8 \$/MWh_{th}, respectively [38], (ix) the prices of cooling and chilled water are 0.273 \$/m³ and 1.0 \$/m³, respectively [4], and (x) the R134a refrigerant cost is 8.1 \$/kg, which was converted from 6.7 €/kg in 2017 [43] using the inflation rate (2%/y) and a USD/EUR exchange rate of 1.1. All prices and costs were based on 2022.

The levelized cost of CO₂ liquefaction (LCCL) was calculated using the total present values of the capital expenditure cost (C_{cap}), debt cost (C_{debt}), and TPC for the plant life (N), which were divided by the total present value of the CO₂ production rate (F_{out}) without impurities:

$$LCCL (\$/t - CO_2) = \frac{\sum_{n=1}^{L_p} \frac{C_{cap,n} + C_{debt,n} + TPC_n}{(1+\gamma)^n}}{\sum_{n=1}^{L_p} \frac{F_{out}}{(1+\alpha)^n}} \quad (1)$$

C_{cap} was given as an annually-equal value of 30% FCI (equity) divided by L_p . C_{debt} was calculated as the fully amortized principal and interest during the life of the plant (L_p). The annual TPC (TPC_n) increased according to the inflation rate (α).

4. Results and Discussion

The CO₂-product at 65 barg and 20 °C satisfied the purity requirements for transportation and sequestration shown in Table 1. The phase envelopes of the CO₂ products obtained from the three feeds were compared, which demonstrated the range of two-phase flow in the *P* and *T* plane. The LCCL was calculated for the CCL processes equipped with a flash or distillation column.

4.1. Process Performance of CCL with Flash or Distillation Column

The product flow rate and purity, CO₂ recovery, as well as the electricity and steam consumptions of the three feeds at a flow rate of 50.068 t/h (or 400, 544 t/y) are listed in Table 3. The product flow rates of the CCL processes with the flash were obtained from a phase equilibrium of a flash at 65 barg and 20 °C, whereas those of the CCL processes with the eight-stage distillation column were obtained from an operating condition achieving a 93% CO₂ recovery. For Feed 1, with a high CO₂ purity of 99.13 vol%, the purity of the product was slightly improved with a 100% recovery using a flash. The product flow rates from the CCL processes with a flash were relatively low for Feeds 2 and 3 owing to their high impurity content of N₂ and H₂, respectively. Liquefied products of 42.9 t/h (97.8 mol% CO₂ and 2.2 mol% N₂) and 33.1 t/hr (98.9 mol% CO₂ and 1.1 mol% H₂) were produced at the bottom of the flash for Feeds 2 and 3, resulting in low CO₂ recoveries.

Table 3. Process performances for CO₂ compression and liquefaction (CCL) with a flash or distillation column from three different CO₂-rich mixtures.

Process Performance		Feed 1		Feed 2		Feed 3	
		Flash	Distil.	Flash	Distil.	Flash	Distil.
Feed	Flow rate (kg/h)	50,068	50,068	50,068	50,068	50,068	50,068
	CO ₂ purity (mol%)	99.13	99.13	97.00	97.00	97.00	97.00
Product	Flow rate (kg/h)	50,038	46,508	42,892	45,735	33,084	46,472
	CO ₂ purity (mol%)	99.28	99.95	97.79	99.81	98.94	99.99
CO ₂ recovery (%)		100.0	93.0	86.1	93.0	66.2	93.0
Electricity consumption (kW _e)	CO ₂ compression	1747	1747	1830	1830	1867	1867
	Cooling utilities	707	1139	648	1204	564	1396
Cooling duty after compressor (kW)		2425	3964	2060	4125	1775	4886
Steam consumption in reboiler (kW _{th})		-	1699	-	1871	-	2608

When the distillation column maintaining a recovery of 93% was used for the removal of impurities, high CO₂ purities of 99.95, 99.81, and 99.99 mol% were achieved for Feeds 1, 2, and 3, respectively, implying that the CCL process with a distillation column can produce CO₂ with a high purity for various feeds with different qualities, unlike a flash.

Feeds 1, 2, and 3 were compressed to 66.2 barg, consuming 1747, 1830, and 1867 kW_e, respectively. When a flash was used, the CO₂ streams after the two-stage compressor entered a cooler to reduce the temperature from 40 to 20 °C, and the heat duties of this cooler were 2.43, 2.06, and 1.78 MW_{th} for Feeds 1–3, respectively, in which the cooling utility system consumed 707, 648, and 564 kW_e of electricity, respectively. When the distillation column was used for Feed 1, chilled water (1539 = 3964 – 2425 kW) was used to cool the top product in the condenser to 17.9 °C and the CO₂ product of the bottom to 20 °C, where 432 kW_e (=1139 – 707 kW_e) of electricity was additionally consumed. The R134a refrigerant was used to cool the top product to 2.7 °C in the condenser and a chiller was used to cool the liquefied CO₂ at the bottom for Feed 2 containing N₂, where an electricity of 556 kW_e (=1204 – 648 kW_e) was required to supply a cooling duty of 2.1 MW (=4.1 – 2.1 MW). Feed 3 containing H₂ required 3.1 MW (=4.9 – 1.8 MW) to decrease the temperature of the top product to 3.3 °C in the distillation column and the CO₂ product at the bottom to 20 °C using the refrigeration cycle and chilled water system, respectively.

Steam was used to evaporate the bottom product in the reboilers of the distillation column. The reboiler temperatures were 26.2, 25.8, and 26.3 °C, where the heat duties were

1.70, 1.87, and 2.61 MW_{th} for Feeds 1–3, respectively. The electricity and heat duty of Feed 3 in the cooling system and reboiler, respectively, were the highest, achieving 93% recovery.

4.2. Phase Envelope for CCL with a Flash or Distillation Column

The phase envelopes on the P and T plane were compared for the pure CO₂, feed without water, and liquefied CO₂ products separated from the flash and distillation columns for Feeds 1–3, as shown in Figures 4–6, respectively. The critical point of pure CO₂ was 31.1 °C and 72.8 barg, which is represented by a single line (thick black solid line) on the phase envelope, as shown in Figure 4. The left side of the single line represents the liquid phase, and the right side represents the gas phase. The phase envelope (thick green solid line) of the liquefied CO₂ product from the distillation column is also a single line because its purity (99.95%) is high. However, the dehydrated Feed 1 (thin blue solid line) and liquefied CO₂ product from the flash (thin red dashed line) indicate two phases at $P = 65$ barg, despite the purity (99.28%) being slightly lower than that of the CO₂ product from the distillation column.

At 65.0 barg, the pure CO₂ and CO₂ product from the distillation column were in the liquid phase below 26.1 °C (inset of Figure 4). The CO₂ product from the flash had a composition of 99.28 mol% CO₂, 0.02 mol% CO, 0.61 mol% H₂, and 0.09 mol% CH₄, demonstrating a two-phase range from 22.8 to 25.3 °C at 65 barg. Assuming that the liquefied CO₂ at 20 °C and 65 barg is transported via a pipeline or ship, the transportation temperature should be below 22.8 and 26.1 °C for the CO₂ products from the flash and distillation columns, respectively. For Feed 1, the operating window of the CO₂ product from the distillation column was approximately 3 °C wider during transportation than that of the CO₂ from the flash.

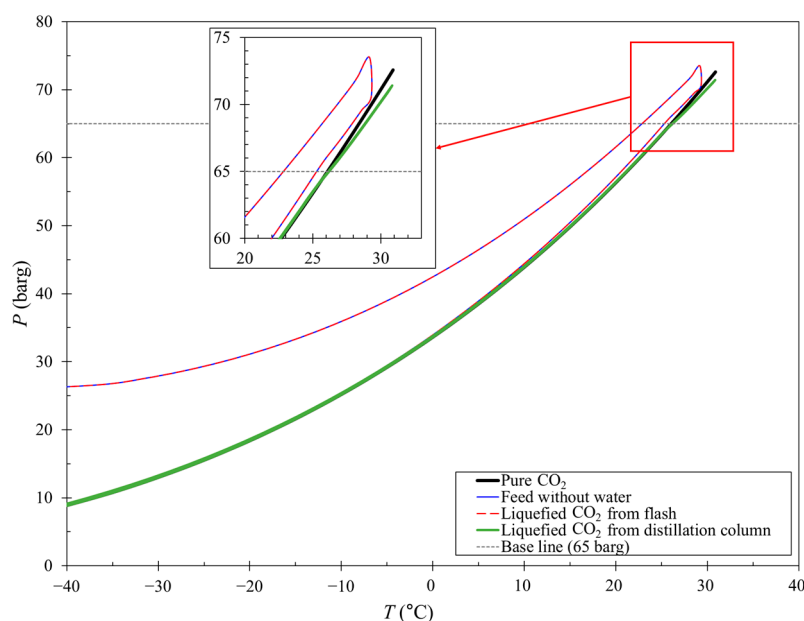


Figure 4. Phase envelopes of pure CO₂, feed without water, and liquefied CO₂ products from the flash and distillation column for Feed 1.

The phase envelopes of the CO₂-rich mixtures from the flash (thin red dashed line) and distillation column (thick green solid line) for Feed 2, which contained 2.9 mol% N₂, are shown in Figure 5. The feed without water (thin blue solid line) at 65 barg has two phases ranging from 17.8 to 23.4 °C, whereas the gas and liquid phases coexist between 19.9 and 24.0 °C for the CO₂ product from the flash (purity = 97.79%), as shown in the inset of Figure 5. The CO₂ product at 65 barg should be transported below 19.9 °C to avoid the gas phase. Because the CO₂ product from the distillation column (purity = 99.81%) does

not exhibit the two-phase region, its temperature window for the liquid transportation is approximately 6 °C wider compared to that of the CO₂ product from the flash.

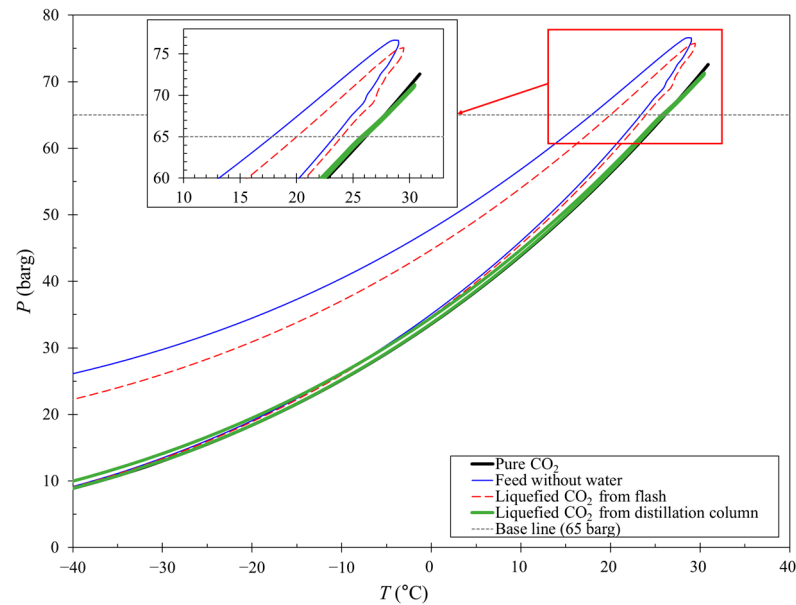


Figure 5. Phase envelopes of the pure CO₂, feed without water, and liquefied CO₂ products from the flash and distillation column for Feed 2.

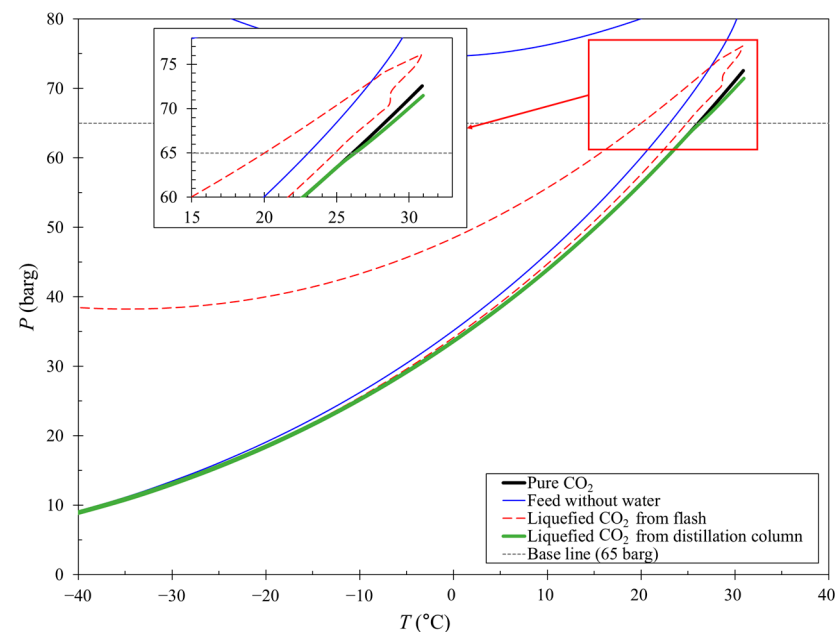


Figure 6. Phase envelopes of the pure CO₂, feed without water, and liquefied CO₂ products from the flash and distillation column for Feed 3.

The gas phase was inevitable for Feed 3 containing 2.9 mol% H₂ (thin blue solid line) at 65 barg. Therefore, the purification of Feed 3 is necessary for liquid transportation at 65 barg. The gas and liquid phases coexist from 19.9 to 24.9 °C for the CO₂ product from the flash (inset of Figure 6). As the CO₂ product from the distillation column had a purity of 99.99 mol%, the two-phase region did not appear at 65 barg. Using a distillation column in the CCL process enables the flexible operation of CO₂ transportation, widening the temperature window in which two-phase flow does not occur.

4.3. Economic Evaluation of CCL with a Flash or Distillation Column

The removal of impurities by the distillation column enhances the operability of CO₂ transportation in the liquid, but increases the capital and production costs in the CCL process. Table 4 presents the TCI, TPC, and LCCL values of the CCL processes for Feeds 1–3.

Table 4. Economic values of the CO₂ compression and liquefaction (CCL) processes with a flash or distillation column.

Economic Values	Feed 1		Feed 2		Feed 3	
	Flash	Distil.	Flash	Distil.	Flash	Distil.
Total capital investment (TCI, M\$)	17.55	20.56	16.00	17.60	15.57	19.44
Total production cost (TPC, M\$/y)	5.96	7.17	5.80	7.10	5.68	7.69
Levelized cost of CO ₂ liquefaction (LCCL, \$/t-CO ₂)	13.24	17.07	14.90	16.90	18.90	18.07

The TCI for the flash separation with Feed 1 was the highest at 17.6 M\$ because the amount of heat required to reduce the temperature to 20 °C was higher than those of Feeds 2 and 3, increasing the equipment cost of the cooling systems. Although the CO₂ compressors consumed less electricity, the utility consumption was the highest, which resulted in the highest TPC (6.0 M\$/yr) for Feed 1.

The TCI and TPC of the CCL processes with the distillation column were higher than those with the flash because the eight-stage distillation column consumed additional steam and refrigerant (or chiller). When the CCL processes with the distillation column were used, the LCCLs increased compared to those with the flash, except for Feed 3, where the LCCL of the CCL process with the flash was higher than that with the distillation column owing to the low recovery (see Eq. (1)). The LCCL of the CCL process with the flash for Feed 1 was the lowest at \$13.2/t-CO₂ owing to the high purity of Feed 1 (99.1%) and high recovery (100%). As the purity of the feed decreased, the LCCL increased, as demonstrated by Feeds 2 and 3.

5. Conclusions

Captured CO₂ containing non-condensable impurities such as N₂ and H₂ can exhibit a two-phase region under certain operating conditions of transportation, injection, and sequestration. In this study, a CO₂ compression and liquefaction (CCL) process with a distillation column was proposed to remove the impurities and avoid an eventual two-phase flow during transportation and storage. The CCL process included a temperature swing adsorption (TSA) for water removal, a two-stage compressor with a cooler, utility systems with a cooling water system, chilled water system, refrigeration cycles, and flash or distillation. The flash was operated at 65 barg and 20 °C, whereas the eight-stage distillation column was operated at a fixed CO₂ recovery of 93%. The Peng–Robinson equation of state (PR EOS) was used to calculate the phase equilibrium, which was in sufficient agreement with the experimental critical points. The phase envelopes of the CO₂ mixtures in the temperature (*T*) and pressure (*P*) plane were obtained using the PR EOS to identify the existence of a two-phase flow. Feed 1 (99.1 mol% CO₂, 1500 ppm H₂O, and 0.7 mol% non-condensable gases), Feed 2 (97.0 mol% CO₂, 1500 ppm H₂O, and 2.85 mol% N₂), and Feed 3 (97.0 mol% CO₂, 1500 ppm H₂O, and 2.85 mol% H₂) were supplied and liquefied at 65 barg and 20 °C.

The CO₂ mixtures obtained through the TSA and flash met the purity requirements for transportation and storage, based on the recommendations reported in the literature. However, when a flash at 65 barg and 20 °C was used, the CO₂ recoveries of Feeds 2 and 3 were low owing to non-condensable impurities (N₂ and H₂). In addition, the flash-separated CO₂ product at 65 barg demonstrated the co-existence of the gas and liquid

phases, restricting the temperature window of liquid CO₂ transportation. Pure CO₂ at 65 barg maintained the liquid phase below 26 °C, whereas the CO₂ products from the flash should be transported below 23 °C for Feed 1 and below 20 °C for Feeds 2 and 3 to avoid a two-phase flow. The CO₂ products from the distillation column exhibited a behavior similar to that of pure CO₂ owing to their high purity. The CCL processes with a distillation column consumed more cooling and heating duties than those with the flash.

The total capital investment (TCI, 17–20 M\$) and total production cost (TPC, 7–8 M\$/y) of the CCL process with the distillation column were higher for Feeds 1–3, compared to the TCI (15–17 M\$) and TPC (5–6 M\$/y) with the flash. The levelized cost of CO₂ liquefaction (LCCL) of the CCL process with the distillation column (17–18 \$/t-CO₂) was higher than that with the flash (13–19 \$/t-CO₂), except for Feed 3, where the recovery was low. Using the distillation column widened the operating temperature window of liquid transportation but increased the LCCL. The CCL process was limited to the CO₂ products at 65 barg. Two-phase flow under various operating conditions during transportation and storage must be investigated. A more rigorous validation of the EOS is also required for the accurate prediction of the phase equilibrium. This study demonstrated that a two-phase flow existed under certain operating conditions, despite the CO₂ purity being high (over 97 mol%), and the distillation column enhanced the operability of liquid CO₂ transportation. The scientific findings will provide a valuable guideline for process design in the field of CCL for CCS.

Author Contributions: Conceptualization: H.K. and H.-M.M. Methodology: S.K. and P.-G.J. Writing—original draft preparation: S.K. Writing—review and editing: Y.-I.L. Supervision: Y.-I.L. Funding acquisition: H.-M.M. All authors have read and agreed to the published version of the manuscript.

Funding: This work was funded by the Korea Institute of Energy Technology Evaluation and Planning (KETEP) (grant no. 20214710100060) by the Korean Government (MOTIE).

Data Availability Statement: Data are contained within the article.

Acknowledgments: We thank Seok-Gyun Yun for his engineering advice and internal communications.

Conflicts of Interest: The authors declare that the research was conducted in the absence of any commercial or commercial or financial relationships that could be construed as a potential conflict of interest.

References

1. IEA. *World Energy Outlook 2020*; International Energy Agency (IEA): Paris, France, 2020.
2. Sun, X.; Shang, A.; Wu, P.; Liu, T.; Li, Y. A review of CO₂ marine geological sequestration. *Processes* **2023**, *11*, 2206. [[CrossRef](#)]
3. Lu, H.; Xin, X.; Ye, J.; Yu, G. Analysis of factors impacting CO₂ assisted gravity drainage in oil reservoirs with bottom water. *Processes* **2023**, *11*, 3290. [[CrossRef](#)]
4. Kim, S.; Lim, Y.I.; Lee, D.; Seo, M.W.; Mun, T.Y.; Lee, J.G. Effects of flue gas recirculation on energy, exergy, environment, and economics in oxy-coal circulating fluidized-bed power plants with CO₂ capture. *Int. J. Energy Res.* **2021**, *45*, 5852–5865. [[CrossRef](#)]
5. Li, H.; Jakobsen, J.P.; Wilhelmsen, Ø.; Yan, J. PVTxy properties of CO₂ mixtures relevant for CO₂ capture, transport and storage: Review of available experimental data and theoretical models. *Appl. Energy* **2011**, *88*, 3567–3579. [[CrossRef](#)]
6. Pal, M.; Karaliūtė, V.; Malik, S. Exploring the potential of carbon capture, utilization, and storage in Baltic sea region countries: A review of CCUS patents from 2000 to 2022. *Processes* **2023**, *11*, 605. [[CrossRef](#)]
7. Abbas, Z.; Mezher, T.; Abu-Zahra, M.R. CO₂ purification. Part I: Purification requirement review and the selection of impurities deep removal technologies. *Int. J. Greenh. Gas Control* **2013**, *16*, 324–334. [[CrossRef](#)]
8. Peletiri, S.P.; Mujtaba, I.M.; Rahmanian, N. Process simulation of impurity impacts on CO₂ fluids flowing in pipelines. *J. Clean. Prod.* **2019**, *240*, 118145. [[CrossRef](#)]
9. Morland, B.H.; Svenningsen, G.; Dugstad, A. The challenge of monitoring impurity content of CO₂ streams. *Processes* **2021**, *9*, 570. [[CrossRef](#)]
10. Li, H.; Wilhelmsen, Ø.; Yan, J. Properties of CO₂ mixtures and impacts on carbon capture and storage. In *Handbook of Clean Energy Systems*; John Wiley & Sons, Ltd.: Hoboken, NJ, USA, 2015; pp. 1–17.
11. Woods, M.; Matuszewski, M. *Quality Guideline for Energy System Studies: CO₂ Impurity Design Parameters*; DOE/NETL-341/011212; National Energy Technology Laboratory (NETL): Pittsburgh, PA, USA; Morgantown, WV, USA, 2013.
12. Hussain, B.Y. *Dynamic Simulations of Carbon Dioxide Pipeline Transportation for the Purpose of Carbon Capture and Storage*. Ph.D. Thesis, University of Birmingham, Birmingham, UK, 2017.

13. Aspelund, A.; Jordal, K. Gas conditioning-The interface between CO₂ capture and transport. *Int. J. Greenh. Gas Control* **2007**, *1*, 343–354. [CrossRef]
14. Porter, R.T.; Fairweather, M.; Pourkashanian, M.; Woolley, R.M. The range and level of impurities in CO₂ streams from different carbon capture sources. *Int. J. Greenh. Gas Control* **2015**, *36*, 161–174. [CrossRef]
15. De Visser, E.; Hendriks, C.; Barrio, M.; Mølnvik, M.J.; De Koeijer, G.; Liljemark, S.; Le Gallo, Y. Dynamis CO₂ quality recommendations. *Int. J. Greenh. Gas Control* **2008**, *2*, 478–484. [CrossRef]
16. Onyebuchi, V.E.; Kolios, A.; Hanak, D.P.; Biliyok, C.; Manovic, V. A systematic review of key challenges of CO₂ transport via pipelines. *Renew. Sust. Energ. Rev.* **2018**, *81*, 2563–2583. [CrossRef]
17. Kahlke, S.-L.; Pampa, M.; Schütz, S.; Kather, A.; Rütters, H. Potential dynamics of CO₂ stream composition and mass flow rates in CCS clusters. *Processes* **2020**, *8*, 1188. [CrossRef]
18. Raimondi, L. CO₂ transportation with pipelines-model analysis for steady, dynamic and relief simulation. *Chem. Eng. Trans.* **2014**, *36*, 619–624.
19. Verma, S.; Oakes, C.; Chugunov, N.; Ramakrishnan, T. Effect of contaminants on the thermodynamic properties of CO₂-rich fluids and ramifications in the design of surface and injection facilities for geologic CO₂ sequestration. *Energy Procedia* **2011**, *4*, 2340–2347. [CrossRef]
20. Brownsort, P.A. *Briefing on Carbon Dioxide Specifications for Transport*. CCUS Projects Network, Norway, EU. 2019. Available online: https://www.ccusnetwork.eu/sites/default/files/TG3_Briefing-CO2-Specifications-for-Transport.pdf (accessed on 29 December 2023).
21. Goos, E.; Riedel, U.; Zhao, L.; Blum, L. Phase diagrams of CO₂ and CO₂-N₂ gas mixtures and their application in compression processes. *Energy Procedia* **2011**, *4*, 3778–3785. [CrossRef]
22. Xu, G.; Liang, F.; Yang, Y.; Hu, Y.; Zhang, K.; Liu, W. An improved CO₂ separation and purification system based on cryogenic separation and distillation theory. *Energies* **2014**, *7*, 3484–3502. [CrossRef]
23. Seo, Y.; Huh, C.; Lee, S.; Chang, D. Comparison of CO₂ liquefaction pressures for ship-based carbon capture and storage (CCS) chain. *Int. J. Greenh. Gas Control* **2016**, *52*, 1–12. [CrossRef]
24. Adu, E.; Zhang, Y.; Liu, D.; Tontiwachwuthikul, P. Parametric process design and economic analysis of post-combustion CO₂ capture and compression for coal-and natural gas-fired power plants. *Energies* **2020**, *13*, 2519. [CrossRef]
25. Deng, H.; Roussanaly, S.; Skaugen, G. Techno-economic analyses of CO₂ liquefaction: Impact of product pressure and impurities. *Int. J. Refrig.* **2019**, *103*, 301–315. [CrossRef]
26. Gong, W.; Remiezowicz, E.; Fosbøl, P.L.; Dlamini, G.M.; von Solms, N. Techno-economic analysis of novel CO₂ liquefaction processes. In Proceedings of the 16th Greenhouse Gas Control Technologies Conference (GHGT-16), Lyon, France, 23–24 October 2022.
27. Øi, L.E.; Eldrup, N.; Adhikari, U.; Bentsen, M.H.; Badalge, J.L.; Yang, S. Simulation and cost comparison of CO₂ liquefaction. *Energy Procedia* **2016**, *86*, 500–510. [CrossRef]
28. Porter, R.T.; Mahgereteh, H.; Brown, S.; Martynov, S.; Collard, A.; Woolley, R.M.; Fairweather, M.; Falle, S.A.E.G.; Wareing, C.J.; Nikolaidis, I.K.; et al. Techno-economic assessment of CO₂ quality effect on its storage and transport: CO2QUEST: An overview of aims, objectives and main findings. *Int. J. Greenh. Gas Control* **2016**, *54*, 662–681. [CrossRef]
29. Zhao, Q.; Li, Y.-X. The influence of impurities on the transportation safety of an anthropogenic CO₂ pipeline. *Process Saf. Environ. Prot.* **2014**, *92*, 80–92. [CrossRef]
30. Martynov, S.; Daud, N.; Mahgereteh, H.; Brown, S.; Porter, R. Impact of stream impurities on compressor power requirements for CO₂ pipeline transportation. *Int. J. Greenh. Gas Control* **2016**, *54*, 652–661. [CrossRef]
31. Ke, J.; Oag, R.M.; King, P.; George, M.W.; Poliakoff, M. Sensing the critical point of high-pressure mixtures. *Angew. Chem. Int. Ed.* **2004**, *43*, 5192–5195. [CrossRef]
32. Venkatarathnam, G. Density marching method for calculating phase envelopes. *Ind. Eng. Chem. Res.* **2014**, *53*, 3723–3730. [CrossRef]
33. Babar, M.; Bustam, M.; Ali, A.; Maulud, A. Identification and quantification of CO₂ solidification in cryogenic CO₂ capture from natural gas. *Int. J. Automot. Mech. Eng.* **2018**, *15*, 5367–5376. [CrossRef]
34. Peletiri, S.P.; Rahmanian, N.; Mujtaba, I.M. Effects of impurities on CO₂ pipeline performance. *Chem. Eng. Trans.* **2017**, *57*, 355–360.
35. Forbes, S.M.; Verma, P.; Curry, T.E.; Friedmann, S.J.; Wade, S.M. *Guidelines for Carbon Dioxide Capture, Transport and Storage*; World Resources Institute: Washington, DC, USA, 2008.
36. Wilson, D.; Basu, R. Thermodynamic properties of a new stratospherically safe working fluid-refrigerant 134a. *ASHRAE Trans.* **1988**, *94*, 2095–2118.
37. Kim, S.; Lim, Y.-I. Heat integration and economic analysis of dry flue gas recirculation in a 500 MW_e oxy-coal circulating fluidized-bed (CFB) power plant with ultra-supercritical steam cycle. *Korean Chem. Eng. Res.* **2021**, *59*, 60–67.
38. Kim, S.; Lim, Y.-I.; Lee, D.; Cho, W.; Seo, M.W.; Lee, J.G.; Ok, Y.S. Perspectives of oxy-coal power plants equipped with CO₂ capture, utilization, and storage in terms of energy, economic, and environmental impacts. *Energy Convers. Manag.* **2022**, *273*, 116361. [CrossRef]
39. Do, T.X.; Mujahid, R.; Lim, H.S.; Kim, J.-K.; Lim, Y.-I.; Kim, J. Techno-economic analysis of bio heavy-oil production from sewage sludge using supercritical and subcritical water. *Renew. Energy* **2020**, *151*, 30–42. [CrossRef]

40. Vu, T.T.; Lim, Y.-I.; Song, D.; Mun, T.-Y.; Moon, J.-H.; Sun, D.; Hwang, Y.-T.; Lee, J.-G.; Park, Y.C. Techno-economic analysis of ultra-supercritical power plants using air-and oxy-combustion circulating fluidized bed with and without CO₂ capture. *Energy* **2020**, *194*, 116855. [[CrossRef](#)]
41. Turton, R.; Bailie, R.C.; Whiting, W.B.; Shaeiwitz, J.A. *Analysis, Synthesis, and Design of Chemical Processes*; Pearson Education: London, UK, 2018.
42. Kemper, J.; Sutherland, L.; Watt, J.; Santos, S. Evaluation and analysis of the performance of dehydration units for CO₂ capture. *Energy Procedia* **2014**, *63*, 7568–7584. [[CrossRef](#)]
43. Botticella, F.; De Rossi, F.; Mauro, A.; Vanoli, G.; Viscito, L. Multi-criteria (thermodynamic, economic and environmental) analysis of possible design options for residential heating split systems working with low GWP refrigerants. *Int. J. Refrig.* **2018**, *87*, 131–153. [[CrossRef](#)]

Disclaimer/Publisher's Note: The statements, opinions and data contained in all publications are solely those of the individual author(s) and contributor(s) and not of MDPI and/or the editor(s). MDPI and/or the editor(s) disclaim responsibility for any injury to people or property resulting from any ideas, methods, instructions or products referred to in the content.